

Effects of Deposited Metallic Silver on Nano-ZnO for the Environmental Purification of Dye Pollutants

Dongfang Zhang*

College of Science, Huazhong Agricultural University, Wuhan 430070, PR China.

Received 14 February 2012, revised 29 February accepted 29 March 2012.

ABSTRACT

Silver-deposited nano-ZnO samples with different Ag loadings were prepared by a one-pot solvothermal method. The structure, physico-chemical and optical properties of the products were characterized by using X-ray diffraction (XRD), scanning electron microscopy (SEM), energy dispersive X-ray analysis (EDS), diffuse reflectance spectroscopy (DRS) and photoluminescence spectra (PLS). The experimental results show that the prepared nanometer zinc oxide powders have a narrow size distribution of 40–60 nm, and their crystal forms can be assigned to hexagonal wurtzite structures. Moreover, the photocatalytic activity of the samples was examined by using photocatalytic oxidation of methylene blue (MB), as a model reaction, and the effects of the noble metal content on the photocatalytic activity were investigated. The results indicate that the photocatalytic activity of the ZnO nanoparticles can be greatly improved by depositing appropriate amounts of noble metal on their surfaces. In addition, a mechanism was proposed in order to account for the enhanced activity. It is evident that the effective lifetime of photogenerated holes is prolonged by electron-trapping of the metallic silver on the surface of the ZnO nanoparticles. The metal deposits serve as electron sinks, which lead to an enhanced rate of dioxygen reduction, facilitating the generation of hydroxyl radicals, and thereby increasing the photocatalytic activity.

KEYWORDS

Noble metal, electron scavengers, heterogeneous photocatalysis.

1. Introduction

Since the early 1970s, steadily worsening environmental pollution and energy shortages have raised awareness of a potential global crisis. Toxic organic compounds, which include some azo dyes, are known to be harmful to human and animal health. Especially, consumer goods which contain aromatic amines originating from azo dyes have been prohibited from manufacture and sale in European Union countries since September 2003 because of its toxicity. For the sustainable development of human society, the development of both pollution-free technologies for environmental remediation and alternative clean energy supplies is an urgent task. Among the wide variety of green earth and renewable energy projects under way, semiconductor photocatalysis has emerged as one of the most promising technologies because it represents an easy way to utilize the energy of either natural sunlight or artificial indoor illumination, which is abundantly available everywhere in the world.

Semiconductor-based photocatalysts have attracted growing interest in the field of environmental applications due to their technological importance and superior properties. Owing to its excellent photofunctional properties, chemical stability, and nontoxic nature, TiO₂ is one of the most used materials for the production of clean energy resources and environmental remediation.^{1–2} As an n-type semiconductor, ZnO is a suitable alternative to TiO₂ as ZnO exhibits better efficiency than TiO₂ in the photocatalytic degradation of organic pollutants and photoelectric conversion.^{3–5} However, the recombination of the photoinduced electrons and holes can occur very quickly, dissipating the input energy as heat. In fact, the separation and recombination of photoinduced charge carriers are in competi-

tion with the photocatalytic reaction, which is only effective when photoinduced electrons and holes are trapped on the surfaces to form active species. Despite the great body of work on semiconductor photocatalysis, the detailed photocatalytic mechanisms and factors affecting the activity are poorly understood. With this background, a study of the effects of phase composition, structure and deposited species, on the properties of photoinduced charges, including charge transfer behaviour and surface states, are relevant to the preparation and application of semiconductor materials. Noble metals like Au and Ag have attracted attention because the collective oscillation of the electrons at the surface, as shown by surface plasmon resonance (SPR), give rise to a wide absorption range in the visible region. Moreover, it is revealed that semiconductor-metal composites enhance the efficiency of the photocatalyst process, wherein metal deposits serve as a passive sink for electrons, hindering their recombination.^{6,7}

In this work, Ag-ZnO composite photocatalyst were successfully prepared by a facile one-pot solvothermal method.⁸ The photocatalytic activities of the Ag-ZnO catalyst was evaluated by measuring decomposition rates of methylene blue (MB). The catalyst was characterized using X-ray diffraction (XRD), scanning electron microscopy (SEM), energy dispersive X-ray analysis (EDS), transmission electron microscopy (TEM), diffuse reflectance spectroscopy (DRS) and photoluminescence spectroscopy (PLS). The goal of this study was to reveal the mechanisms of photocatalytic activity enhancement by investigating the effects of silver on the photoinduced charge property and photocatalytic activity of ZnO nanoparticles. This is valuable for the practical application of ZnO in the field of photocatalysis, and will help to understand the photophysical and photochemical processes.

* E-mail: zdfbb@yahoo.cn

2. Experimental

2.1 Catalyst Preparation

All the reagents were analytical grade and were used as such without any further purification. Deionized water that was prepared by an ultra pure water system type smart-2-pure (TKA Ltd, Germany) was used throughout. Silver-deposited ZnO nanocrystals were prepared by a one-pot, hydrothermal method. The reactions were carried out in a Teflon-lined stainless steel autoclave with a capacity of 200 mL. In brief, it involved the addition of 80 mL of a 4 mmol zinc sulfate heptahydrate ($\text{ZnSO}_4 \cdot 7\text{H}_2\text{O}$) solution in 2-propanol [$(\text{CH}_3)_2\text{CHOH}$, Aldrich, 99.5 atom% purity] under vigorous stirring at room temperature, to 150 mL of 6 mmol hexamethylenetetramine ($\text{C}_6\text{H}_{12}\text{N}_4$), and the required amount of silver nitrate (AgNO_3) to get Ag-ZnO powders with different Ag loadings (0.0, 11.5, 23 and 34.5 mg, mass ratio: 0.0–3.0 wt%). Thereafter, the solution was transferred into a Teflon-lined stainless steel autoclave. The autoclave was sealed and heated, in a temperature-controlled oven, at 200 °C for 10 h and then cooled to room-temperature naturally. The products were centrifuged, washed respectively with absolute ethanol and deionized water three times, and finally dried under vacuum at 80 °C for 5 h. The role of the hexamethylenetetramine is to provide weakly basic conditions under which, $\text{Zn}(\text{OH})_2$ precipitates. In the autoclave, the $\text{Zn}(\text{OH})_2$ is then converted to ZnO, and the usage of crystalline photocatalysts will be attractive in an online system of photo-degradation processes.

2.2 Catalyst Characterization

X-ray powder diffraction (XRD) data were recorded at room temperature with an X-ray diffractometer (XRD-6000, Shimadzu Corporation) using $\text{Cu K}\alpha$ irradiation ($\lambda = 0.15408 \text{ nm}$), operated at 40 kV and 100 mA. The morphology of the acquired samples were investigated using a JEOL JSM-6700F SEM microscope equipped with an energy dispersive X-ray spectrometer. The percentage of UV-vis reflectance of the catalysts was measured by diffuse reflectance spectroscopy (DRS) of the powdered form of the catalysts using a Scan UV-vis-NIR spectrophotometer (Varian Cary 500) in the region 200–800 nm. The spectrophotometer was equipped with an integrating sphere assembly and polytetrafluoroethylene was used as reflectance material in

the UV-vis absorbance experiment. The photoluminescence (PL) emission spectra of the samples were measured at room temperature using an LS-55 spectrometer (PerkinElmer) illuminated with a 325-nm He-Cd laser as an excitation source.

2.3 Evaluation of Photocatalytic Activity

The photocatalytic activity of the ZnO nanoparticles prepared above was tested using the degradation of aqueous methylene blue (MB: $\text{C}_{16}\text{H}_{18}\text{ClN}_3\text{S}$, Alfa Aesar) solutions, and photo-degradation of MB, which is a typical dye resistant to biodegradation, has been studied. The artificial light photocatalytic activity test was conducted in a quartz photoreactor with a cylindrical configuration. A mixture of 200 mL of 100 ppm aqueous MB and 200 mg of Ag-deposited ZnO or pure ZnO powders were firstly stirred for 30 min in a quartz beaker in the dark to establish an adsorption/desorption equilibrium for model pollutant and dissolved oxygen on the surface of the ZnO. Thereafter, the suspension was continuously agitated while being irradiated by a 380-W UV lamp ($\lambda_{\text{max}} = 365 \text{ nm}$). The distance between the light and the suspension was kept at 10 cm. During the irradiation experiments, 5 mL samples were withdrawn from the suspension at given intervals and immediately centrifuged at 5000 rpm for 10 min to remove solids. The concentration of MB remaining in solution after illumination was determined spectrophotometrically at a wavelength of 661.0 nm. The decolorization efficiency of the MB was determined by the formula: $\text{Decolorization} = (C_0 - C)/C_0$, where C_0 , C represents the concentration of the initial and remaining MB.

3. Results and Discussion

A representative XRD pattern of ZnO/Ag nano-particles (2.0 wt% Ag) is shown in Fig. 1. The diffraction peaks appearing at 31.7, 34.4, 36.2, 47.4, 56.5, 62.7, 66.3, 67.8 and 69.1° match the crystal plane of a wurtzite structure of ZnO and are comparable to literature values, JCPDS (PDF: #36-1451). Furthermore, all diffraction peak positions of ZnO in ZnO/Ag composite accord with that of pure ZnO, indicating that Ag did not incorporate into the lattice of ZnO but dispersed on the surface of the ZnO nanoparticles. Therefore, the deposition of Ag does not affect the crystal or phase structure of ZnO. Metal islands deposited on the semiconductor surface have been shown to effectively trap the electrons promoted to the conduction band and thus the free

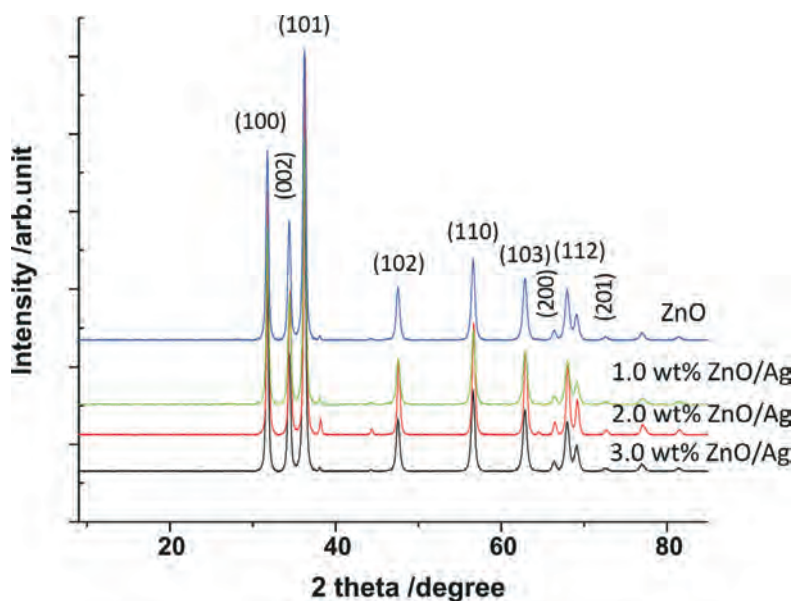


Figure 1 The XRD patterns of bare ZnO and Ag-coated ZnO nanoparticles.

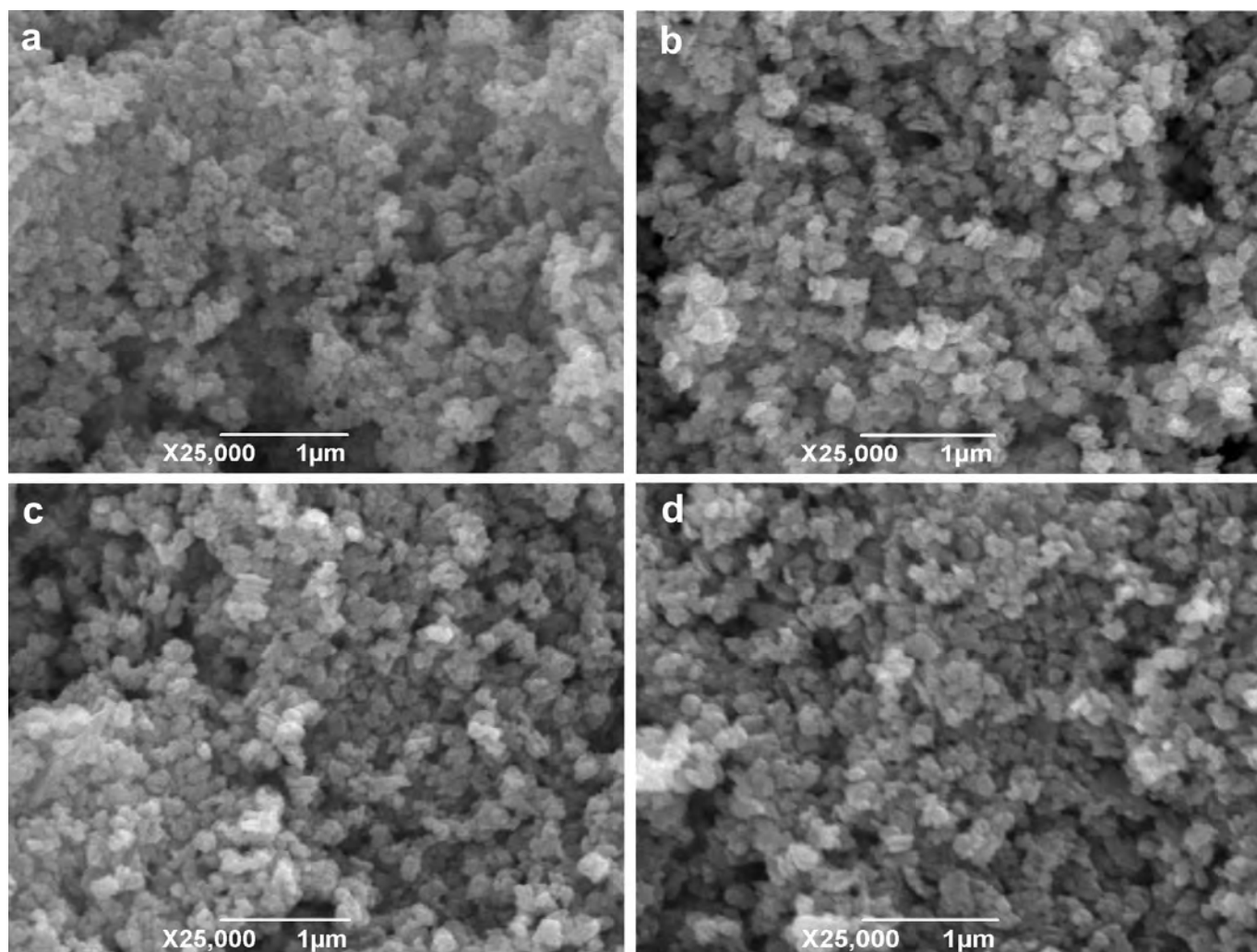


Figure 2 Representative SEM images of Ag-coated ZnO nanoparticles, with (a) 0.0 wt%, (b) 1.0 wt%, (c) 2.0 wt% and (d) 3.0 wt% Ag loading.

holes formed in the valence band can participate in oxidation reactions. The crystal sizes of all of the samples were estimated using the Scherrer equation: $D = m\lambda/\text{acos}\Phi$, where a represents the half-height width of the diffraction peak of, $m = 0.89$ is a coefficient, Φ is the diffraction angle, and λ is the X-ray wavelength corresponding to the Cu $K\alpha$ irradiation. The average sizes of the ZnO/Ag nanoparticles, calculated by the Scherrer formula, were estimated to be between 14 and 20 nm. The crystal size of the samples are calculated to be about 19.8, 18.2, 16.9 and 15.2 nm for pure ZnO, 1.0 wt%, 2.0 wt% and 3.0 wt% ZnO/Ag, respectively. The size decrease could be caused by lattice deformation associated with oxygen vacancies in the anatase crystallites, which may hinder crystallite growth. Nonetheless, there is no remarkable change in the d space values, which implies that the noble metal silver modification does not change the average unit cell dimension in deposited samples. The absence of reflection from the silver deposits can be attributed to the low percentage deposition. The X-ray powder diffraction technique is unable to detect impurity or crystalline phase percentages lower than 5 %.

The ZnO/Ag nano-particles were further characterized using SEM. The SEM images of the 0.0 wt%, 1.0 wt%, 2.0 wt%, 3.0 wt% ZnO/Ag composites are shown in Fig. 2. It can be seen that a large number of uniform nanospheres with diameters of about 50 nm were formed. The aggregate size of the ZnO/Ag samples was notably larger than that of pure the ZnO crystals. Furthermore, the surfaces of the nanospheres are rough, with

many pores, which indicates that these nanospheres are not solid particles but are composed of small nanoparticles. The presence of unique structures suggests that the inherent porosity originates from aggregated nanoparticles. The porosity of the nanocomposite creates many nanochannels, which enable an intimate contact between innocuous species and the ZnO nanoparticles. Such an intimate contact between deposited silver particles and zinc oxide might be important to the synergistic effect or to the interparticle charge migration because metallic silver can act as an electron acceptor which reduces the rate of electron-hole recombination. The observed size of composite particles is not consistent with XRD analysis. The deviation may arise from the following reason: the XRD estimated value is the size of single crystallites, while the SEM measured value is the size of agglomerates.

EDS spectra were utilized to characterize the composition of the nanospheres. Spectra were recorded at various positions on a 2 % ZnO/Ag nanosphere, as shown in Fig. 3. It can be seen that the sample is mainly composed of Ag, Zn and O elements. The percentage composition of these elements is different at different positions, which shows that the deposition of Ag is not uniform on the surface of the nanospheres. There was no evidence of other impurities present in the ZnO/Ag composite.

The UV-vis diffuse reflectance spectra of the prepared samples were recorded to obtain insight into their light absorption characteristics and the interactions of the photocatalytic materials (e.g. ZnO) with photon energies directly. A typical results is shown

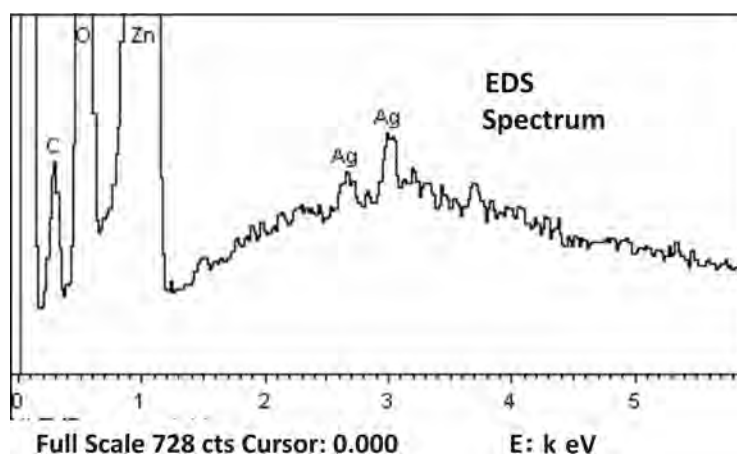


Figure 3 Representative EDS patterns of a 2.0 wt% ZnO/Ag nanoparticle.

in Fig. 4. As a photocatalyst, the wavelength distribution of the absorbed light is one of the important properties regardless of the quantum yield. From this point, the high photoactivity of silver-deposited samples can be attributed to the higher UV-vis light absorbance, as shown by the UV-vis diffuse reflectance spectra. In Fig. 4, UV-vis spectra of 0.0 wt%, 1.0 wt%, 2.0 wt% and 3.0 wt% ZnO/Ag specimens are shown. It can be seen that all the samples have a strong absorption between 300 to 400 nm. The absorption wavelength maximum decreases with an increase in Ag content, but the absorption intensity increases. These facts indicate that the photocatalytic oxidation power of the catalysts will increase since the band gap energy increases and so the redox potential will increase correspondingly. This should produce a more powerful oxidative reaction species. At the same time, the quantum yield will increase since the absorption ability increases with an increase in the Ag loading.

A semiconductor is characterized by the electronic band structure of the highest occupied molecular orbital (HOMO), also called the valence band (VB), and the lowest unoccupied molecular orbital (LUMO), also called the conduction band (CB). The energy difference between the HOMO and LUMO levels is regarded as the band gap energy (E_g).⁹⁻¹² Only an excitation energy higher or equal to the band gap energy of the semiconductor, can photogenerated charge carriers (excited electrons and holes).

However, the excited electrons in the CB easily return to the VB by a recombine with the holes. During the recombination of photogenerated charge carriers, a certain amount of chemical energy will be released, which will further transform, possibly into heat or to light energy. The light energy can be dissipated as radiation, which results in a luminescence emission of semiconductor material, called the photoluminescence (PL) phenomenon of the semiconductor. In this regards, the photoluminescence (PL) emission spectrum is useful to investigate the efficiency of charge carrier trapping, migration and transfer, and to understand the fate of electron-hole pairs in semiconductor particles. For nanostructured materials, the PL spectra are related to the transfer behaviour of the photo-induced electrons and holes so that it can be used to evaluate the recombination rate of charge carriers. Figure 5 shows the PL spectra of the prepared samples at room temperature. There is one strong peak in the wavelength range from 440 to 500 nm. This PL signal is attributed to excitonic PL, and the intensity of this signal varies in the following order: pure ZnO > 1.0 wt% ZnO/Ag > 3.0 wt% ZnO/Ag > 2.0 wt% ZnO/Ag. Since the PL emission results from the recombination of photo-induced electrons and holes, the lower PL intensity means a lower recombination rate of electrons and holes. Pure ZnO has the greatest relative intensity emission spectrum, which means that the electrons and holes in the single

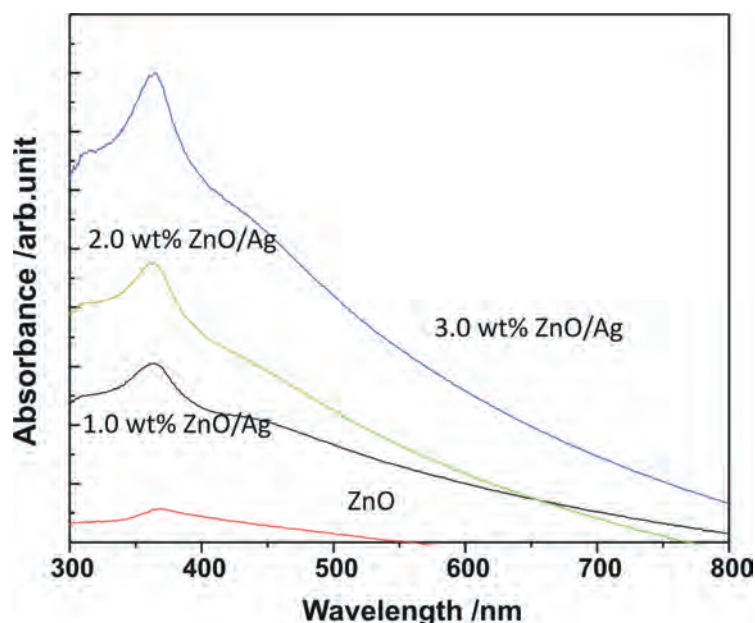


Figure 4 UV-vis spectra of the ZnO/Ag samples.

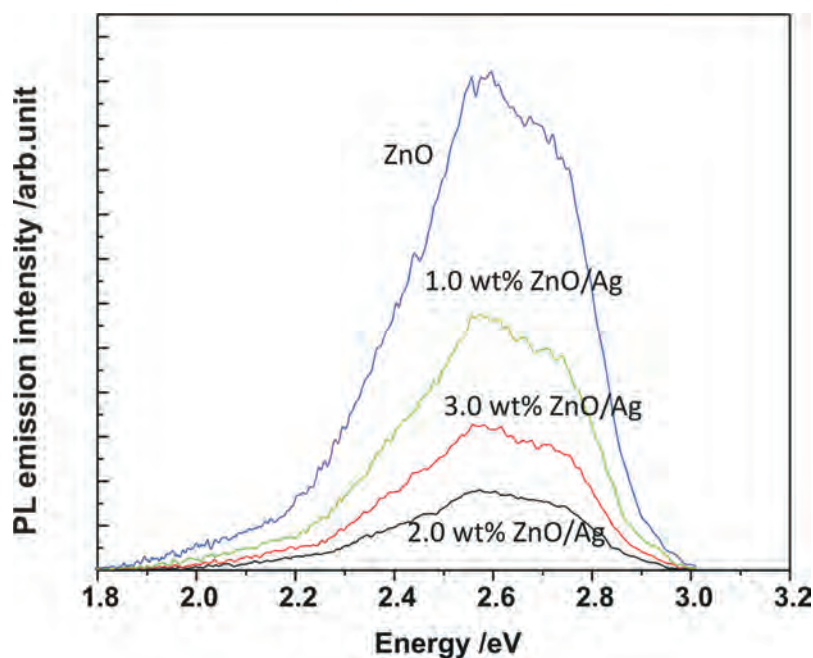


Figure 5 The PL spectra of the ZnO/Ag samples.

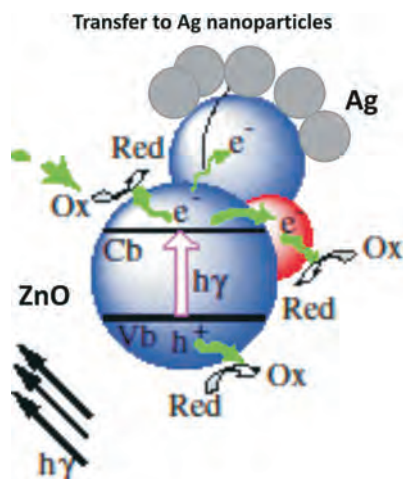


Figure 6 A schematic representation of charge separation and interfacial redox reactions at the metallic Ag-modified ZnO composites.

ZnO matrix are easy to recombine. The recombination probability is basically reduce with the increase in the amount of Ag deposited. Figure 6 shows how the formation of a Schottky barrier at the ZnO-Ag interface restrains the recombination of electrons and holes. At higher Ag concentrations, the Ag sites could serve as recombination centres. An optimal amount of Ag content is 2.0 wt% Ag.

The photocatalytic activity of the ZnO/Ag composites were evaluated under UV light. The decomposition of MB, after illumination for 80 min, was 25.07 %, 63.51 %, 82.90 % and 68.47 %, respectively, for pure ZnO, 1.0 wt%, 2.0 wt% and 3.0 wt% ZnO/Ag nanoparticles. Clearly, the optimal Ag loading is 2 wt%. This is consistent with results described previously.^{13–16} In conclusion, the electron trapping effect of Ag is favourable for the improvement of the photocatalytic activity of ZnO due to the enhancement of the separation efficiency of photogenerated electrons and holes.^{17,18} The considerable decrease of the visible PL emissions indicates that the surface defects in the ZnO photocatalyst are greatly reduced after the Ag loading, suggesting that the metallic Ag is deposited on the defect sites, which is

in agreement with the results obtained from the PL spectra. Furthermore, the deposited silver increases the rate of electron transfer to dissolved oxygen. However, silver particles may act as recombination centres at high silver deposition, which is caused by the electrostatic attraction of negatively charged silver and positively charged holes. Therefore, high amounts of Ag may not be very useful for improving the photocatalytic activity.

4. Conclusion

In summary, this paper presents the preparation of ZnO/Ag nanophotocatalyst and its application in the mineralization of pollutant dye molecules. The experimental result shows that the prepared nanometer zinc oxide powders have a narrow size distributions of about 30 nm, and their crystal forms can be ascribed to a hexagonal system. The strongest absorption wavelength decreases, but the absorption intensity increases with an increase of Ag loading. The photocatalytic activity of ZnO/Ag was tested with the photocatalytic degradation of MB. The results indicated that the photocatalytic activity of ZnO nanoparticles can be greatly improved by depositing appropriate amounts of silver on the surface. The photoluminescence and photodegradation properties of ZnO/Ag nanocomposites means that they could be used in the purification of polluted water or air. Furthermore, it is believed that this synthetic approach could be used to fabricate other metallic oxide/metal nanostructures.

Acknowledgements

This work was supported by the Fundamental Research Funds of the Central Universities and Huazhong Agricultural University Scientific & Technological Self-innovation Foundation (2009QC016) and the Hubei Provincial Natural Science Foundation of China (2011CDB148).

References

- 1 B. Tryba, P. Brożek, M. Piszcz and A.W. Morawski, *Pol. J. Chem. Tech.*, 2011, **13**, 8–14.
- 2 T. Bunhu, A. Kindness and B.S. Martincigh, *S. Afr. J. Chem.*, 2011, **64**, 139–143.
- 3 D.F. Zhang, *Russ. J. Phys. Chem. A.*, 2012, **86**, 93–99.

- 4 V. Srikant and D. Clarke, *J. Appl. Phys.*, 1998, **83**, 5447–5451.
- 5 V. Kandavelu, H. Kastien and T. Ravindranathan, *Appl. Catal. B.*, 2004, **48**, 101–111.
- 6 D.F. Zhang, *Russ. J. Phys. Chem. A.*, 2012, **86**, 498–503.
- 7 D.F. Zhang, *High. Energ. Chem.*, 2012, **46**, 133–138.
- 8 J. Yu and X. Yu, *Environ. Sci. Technol.*, 2008, **42**, 4901–4907.
- 9 Q. Xiao, Z. Si, Z. Yu and G. Qiu, *Mater. Sci. Eng. B.*, 2007, **137**, 189–194.
- 10 Q. Xiao, Z. Si, J. Zhang, C. Xiao and X. Tan, *J. Hazard. Mater.*, 2008, **150**, 62–67.
- 11 Q. Xiao, Z. Si, Z. Yu and G. Qiu, *J. Alloys Comp.*, 2008, **450**, 426–431.
- 12 J. Shi, J. Chen, Z. Feng, T. Chen, Y. Lian, X. Wang and C. Li, *J. Phys. Chem. C.*, 2007, **111**, 693–699.
- 13 J. Sun, L. Gao and Q. Zhang, *J. Am. Ceram. Soc.*, 2003, **86**, 1677–1681.
- 14 C. Su, B. Hong and C. Tseng, *Catal. Today.*, 2004, **96**, 119–126.
- 15 B.M. Sergeev and G.B. Sergeev, *Colloid. J.*, 2010, **72**, 145–148.
- 16 D. Lin, H. Wu, W. Zhang, H. Li and W. Pan, *Appl. Phys. Lett.*, 2009, **94**, 172103–172105.
- 17 O.V. Dementeva and V.M. Rudoy, *Colloid. J.*, 2011, **73**, 724–742.
- 18 R. Georgekutty, M. Seery and S. Pillai, *J. Phys. Chem. C.*, 2008, **112**, 13563–13570.